The Journal of Immunology

IκB Kinase Complex α Kinase Activity Controls Chemokine and High Endothelial Venule Gene Expression in Lymph Nodes and Nasal-Associated Lymphoid Tissue

Danielle L. Drayton, Giuseppina Bonizzi, Xiaoyan Ying, Shan Liao, Michael Karin and Nancy H. Ruddle

J Immunol 2004; 173:6161-6168; ;
doi: 10.4049/jimmunol.173.10.6161
http://www.jimmunol.org/content/173/10/6161

The Journal of Immunology is published twice each month by
The American Association of Immunologists, Inc.,
1451 Rockville Pike, Suite 650, Rockville, MD 20852

Print ISSN: 0022-1767 Online ISSN: 1550-6606.

IκB Kinase Complex α Kinase Activity Controls Chemokine and High Endothelial Venule Gene Expression in Lymph Nodes and Nasal-Associated Lymphoid Tissue[1]

Danielle L. Drayton,* Giuseppina Bonizzi,† Xiaoyan Ying,* Shan Liao,* Michael Karin,† and Nancy H. Ruddle[2]*

The lymphotoxin (LT) β receptor plays a critical role in secondary lymphoid organogenesis and the classical and alternative NF-κB pathways have been implicated in this process. IKKα is a key molecule for the activation of the alternative NF-κB pathway. However, its precise role and target genes in secondary lymphoid organogenesis remain unknown, particularly with regard to high endothelial venules (HEV). In this study, we show that IKKα^{AA} mutant mice, who lack inducible kinase activity, have hypocellular lymph nodes (LN) and nasal-associated lymphoid (NALT) tissue characterized by marked defects in microarchitecture and HEV. In addition, IKKα^{AA} LNs showed reduced lymphoid chemokine CCL19, CCL21, and CXCL13 expression. IKKα^{AA} LN- and NALT-HEV were abnormal in appearance with reduced expression of peripheral node addressin (PNAd) explained by a severe reduction in the HEV-associated proteins, glycosylation-dependent cell adhesion molecule 1 (GlyCAM-1), and high endothelial cell sulfotransferase, a PNAd-generating enzyme that is a target of LTαβ. In this study, analysis of LTβ$^{-/-}$ mice identifies GlyCAM-1 as another LTβ-dependent gene. In contrast, TNFRI$^{-/-}$ mice, which lose classical NF-κB pathway activity but retain alternative NF-κB pathway activity, showed relatively normal GlyCAM-1 and HEC-6ST expression in LN-HEV. In addition, in this communication, it is demonstrated that LTβR is prominently expressed on LN- and NALT-HEV. Thus, these data reveal a critical role for IKKα in LN and NALT development, identify GlyCAM-1 and high endothelial cell sulfotransferase as new IKKα-dependent target genes, and suggest that LTβR signaling on HEV can regulate HEV-specific gene expression. ***The Journal of Immunology,*** **2004, 173: 6161–6168.**

Signaling by lymphotoxin (LT)[3]α or TNF-α through the TNFRI (p55) and LTαβ heterodimers through the LTβR is of critical importance in inflammation and secondary lymphoid organogenesis (spleen, Peyer's patch (PP), nasal-associated lymphoid tissue (NALT), and lymph node (LN)). TNFRI-deficient mice exhibit normal LNs, reduced numbers of PP, and mild splenic microarchitecture defects (1, 2), whereas LTβR-deficient mice are characterized by a more severe phenotype—a complete absence of all LNs, PP, and marked splenic abnormalities (3). LTα$^{-/-}$ mice also lack all LNs and PPs (4, 5) and exhibit severe splenic defects, while TNF-α$^{-/-}$ mice retain all LNs and PP and have limited defects in LN and splenic architecture (2, 6). Given the relatively mild defects in TNF-α$^{-/-}$ mice, the phenotype of TNFRI$^{-/-}$ mice does not reflect signaling from TNF-α only but suggests an important role for LTα:TNFRI interaction in secondary lymphoid organogenesis. LTβ$^{-/-}$ mice lack PP and peripheral LNs (PLNs) but retain mesenteric LNs (MLN) and cervical LNs, and exhibit splenic defects that are less severe than those of LTα$^{-/-}$ mice (7).

Two NF-κB signaling pathways, the canonical and alternative pathways that can be activated in response to TNFR1 or LTβR engagement, have been implicated in differential regulation of secondary lymphoid organogenesis (8). Additional TNF family receptors, B cell-activating factor (BAFF)-R and CD40, also appear to participate in the alternative pathway (9). In mammals, the NF-κB family of transcription factors includes five members that form various homo- and heterodimeric complexes: NF-κB1 (p105 processed to p50), NF-κB2 (p100 processed to p52), RelA (p65), RelB, and c-Rel (9). Activation of the canonical NF-κB pathway can be induced by a wide variety of stimuli including proinflammatory cytokines, such as IL-1 and TNF-α, bacterial endotoxins, and viral proteins (10). In most cell types, NF-κB is sequestered in the cytoplasm by inhibitory IκB proteins. Activation of NF-κB depends on the IκB kinase complex (IKK), which contains the IKKγ regulatory subunit and two catalytic subunits, IKKα and IKKβ (9). IKKβ and IKKγ are critical mediators of the canonical NF-κB pathway required for phosphorylation of IκB proteins, whereas IKKα is dispensable for activation of this pathway in response to most stimuli (10–12). Following IKK activation, the IκB proteins are phosphorylated and degraded through a ubiquitin-dependent process, thereby allowing nuclear translocation of NF-κB dimers that activate expression of proinflammatory genes, including VCAM, MIP-1β, and MIP-2 (8, 9).

*Department of Epidemiology and Public Health, Section of Immunobiology, Yale University School of Medicine, New Haven, CT 06520; and †Laboratory of Gene Regulation and Signal Transduction, Department of Pharmacology, University of California, San Diego, La Jolla, CA 92093

Received for publication July 9, 2004. Accepted for publication September 10, 2004.

The costs of publication of this article were defrayed in part by the payment of page charges. This article must therefore be hereby marked *advertisement* in accordance with 18 U.S.C. Section 1734 solely to indicate this fact.

[1] This work was supported by National Institutes of Health Grants RO1 CA 16885 (to N.H.R.), DK 57731 (to N.H.R.), F31 GM 20919 (to D.L.D.), and AI434477 (to M.K.). M.K. is an American Cancer Society Research Professor.

[2] Address correspondence and reprint requests to Dr. Nancy H. Ruddle, Yale University School of Medicine, Department of Epidemiology and Public Health, 60 College Street, P.O. Box 208034, New Haven, CT 06520-8034. E-mail address: nancy.ruddle@yale.edu

[3] Abbreviations used in this paper: LT, lymphotoxin; PP, Peyer's patches; NALT, nasal-associated lymphoid tissue; LN, lymph node; CD62L, L-selectin; BAFF, B cell-activating factor; IKK, IκB kinase complex; IKKα^{AA}, IKKα kinase inactive; NIK, NF-κB inducing kinase; MLN, mesenteric lymph node; HEV, high endothelial venule; HEC-6ST, high endothelial cell sulfotransferase; PNAd, peripheral node addressin; GlyCAM-1, glycosylation-dependent cell adhesion molecule 1; DIG, digoxigenin; WT, wild type; FDC, follicular dendritic cell; PLN, peripheral lymph node.

0022-1767/04/$02.00

LT$\alpha\beta$ binding to LTβR results in activation of the canonical NF-κB pathway as well as the alternative NF-κB pathway. The latter is based on phosphorylation-dependent proteolytic processing of cytosolic NF-κB2 (p100) to p52 and nuclear translocation of p52:RelB heterodimers (8, 9, 13–15). Activation of the alternative pathway requires the NF-κB-inducing kinase (NIK) and IKKα, but is independent of IKKβ and IKKγ (8, 13, 16). Early studies in embryonic fibroblasts from alymphoplasia mice (*aly/aly*), which lack functional NIK (17), and from IKK$\alpha^{-/-}$ mice revealed that NIK and IKKα are dispensable for TNFRI-induced NF-κB activation but are required for activation of the alternative NF-κB pathway in response to LTβR engagement (14). Other studies have demonstrated that LTβR-induced NF-κB2 processing and RelB nuclear translocation are NIK- and IKKα-dependent (8, 16). Early data implicated both the canonical and alternative NF-κB pathways in control of lymphoid chemokine expression— CCL19 (EBV-induced molecule 1 ligand chemokine), CCL21 (secondary lymphoid chemokine), and CXCL13 (B lymphocyte chemoattractant; Ref. 18). More recent results derived from the activation of the LTβR in vivo by treatment of mice with an LTβR agonistic reagent suggests that the LTβR→NIK→IKKα alternative pathway induces expression of these lymphoid chemokine genes (8). Furthermore, studies in LTβ-deficient and rat insulin promoter LT$\alpha\beta$ transgenic mice indicate an involvement of LTβR signaling in regulation of high endothelial venule (HEV)-specific gene expression (19). Though the classical NF-κB pathway has been analyzed in endothelial cell lines in vitro, the roles of the classical and alternative NF-κB pathways in HEV in vivo is completely unknown. This is the major focus of the present communication.

HEV are specialized postcapillary venules that facilitate L-selectin $(CD62L)^+$ lymphocyte extravasation into LN and NALT through expression of adhesion molecules, peripheral node addressin (PNAd), and lymphoid chemokines. PNAd, a CD62L ligand detected by the MECA 79 Ab, is generated by high endothelial cell sulfotransferase (HEC-6ST)-mediated sulfation of various glycoproteins including CD34 and glycosylation-dependent cell adhesion molecule 1 (GlyCAM-1; Ref. 20). In the absence of HEC-6ST, the normal luminal MECA 79 staining pattern is lost, though abluminal staining remains (20). Although the LTα:TNFRI system can regulate mucosal addressin cell adhesion molecule 1 expression (21–23), presumably through the canonical NF-κB pathway, our previous data suggest that the LT$\alpha\beta$:LTβR system is a key regulator of PNAd through induction of HEC-6ST (19). One hypothesis to be tested in this study is that this occurs through the alternative NF-κB pathway.

Analysis of *aly/aly* mice or mice with targeted disruptions of alternative NF-κB pathway genes, including NIK, NF-κB2, and RelB have revealed important roles for all of these molecules in the generation of normal splenic microarchitecture and PP development (24). *Aly/aly* and NIK$^{-/-}$ mice lack all LNs, while mice deficient in the downstream molecules, RelB and NF-κB2, have a less profound defect in that they lack some, but not all LNs (24, 25). A role for IKKα in LN organogenesis has not been established. IKK$\alpha^{-/-}$ mice exhibit perinatal death associated with defects in skeletal morphogenesis and epidermal differentiation (26, 27). Given the complete absence of LNs in NIK$^{-/-}$ mice, the relative paucity of LNs in RelB$^{-/-}$ and NF-κB2$^{-/-}$ mice, and IKKα perinatal lethality, studies addressing the role of these molecules in secondary lymphoid organogenesis have focused on PP and spleen development and have revealed the absence of PP and multiple splenic defects (24).

The NALT is an organized lymphoid tissue found in the rodent nasal tract that has structural similarities to PPs as well as the tonsils and adenoids in humans due to its common origin from the Waldeyer's ring (28). Previous studies have demonstrated that initiation of NALT organogenesis is independent of LTα, LTβ, LTβR, and NIK, NF-κB2, and RelB. However, the NALT of mice deficient in these molecules exhibit reduced cellularity and diminished expression of lymphoid chemokines and vascular addressins (24, 29). To address the contribution of the alternative NF-κB pathway to LN and NALT organogenesis, particularly the role of IKKα in these processes, we have studied IKKα^{AA} mutant mice, in which two amino acid substitutions were introduced into the activating phosphorylation sites of IKKα, resulting in prevention of its activation by upstream stimuli (30). IKKα^{AA} mice are viable and display only minor developmental defects (30). In regard to lymphoid organ development, IKKα^{AA} mice were found to lack PP and exhibit defects in splenic organization similar to IKK$\alpha^{-/-}$ mice (13).

In this study, we provide in vivo evidence that IKKα kinase activity is required for normal LN and NALT organogenesis through regulation of tissue microarchitecture, cellular composition, lymphoid chemokine expression, and HEV-specific gene expression. In addition to highlighting a role for IKKα kinase activity in LN and NALT organogenesis, these studies identify GlyCAM-1 and HEC-6ST as new IKKα-dependent target genes.

Materials and Methods

Mice

TNFRI$^{-/-}$ mice were purchased from The Jackson Laboratory (Bar Harbor, ME). LT$\beta^{-/-}$ mice have been previously described (31). TNFRI$^{-/-}$ and LT$\beta^{-/-}$ mice, on a C57BL/6 background, were studied under a protocol approved by the Yale University Institutional Animal Care and Use Committee. IKKα^{AA} mice, on a 129/C57BL/6 genetic background, were previously described (30) and studied under a standard protocol approved by the University of California, San Diego, Office of Animal Care (La Jolla, CA) according to National Institutes of Health guidelines. All mice were studied between 6 and 10 wk of age.

LN visualization

Adult mice were injected in the hind footpads with 10 μl of 1% Evans blue in PBS (Eastman Kodak, Rochester, NY) 24 h before sacrifice. The dye becomes concentrated within lymphoid tissue and facilitates macroscopic detection of even very small LNs.

Histologic analysis

For immunofluorescence, LN and NALT tissues were dissected and frozen in OCT compound (Tissue-Tek; Sakura Finetek, Torrance, CA) on dry ice. NALT tissue was isolated as previously described (32). Seven-micrometer tissue sections were cut (longitudinal sections of NALT tissue) onto poly-L-lysine-coated glass slides (Sigma-Aldrich, St. Louis, MO), fixed in 100% cold acetone for 10 min, and stored at −70°C. For staining, slides were air-dried at room temperature. Sections were double-stained with anti-HEC-6ST generated by our laboratory (19) and MECA 79 (anti-PNAd; BD Pharmingen, San Diego, CA) as previously described (19), or with MECA 79 and anti-LTβR (BD Pharmingen) Abs. For MECA 79 and LTβR double-staining, MECA 79 was detected using Cy3-conjugated goat anti-rat IgM Ab (Jackson ImmunoResearch Laboratories, West Grove, PA), and LTβR was detected using biotinylated anti-hamster IgG (Jackson ImmunoResearch Laboratories) secondary Ab followed by incubation with Cy2-conjugated streptavidin (Jackson ImmunoResearch Laboratories). Slides were analyzed by fluorescence microscopy using a Zeiss Axioskop microscope (Carl Zeiss Microimaging, Thornwood, NY).

For immunohistochemistry, frozen sections of LN tissue were prepared and stained as previously described (19). Primary Abs used were as follows: anti-CD35 (CR1) from BD Pharmingen, and rabbit-anti-mouse GlyCAM-1 (CAM 02) was a generous gift from Dr. S. Rosen (University of California, San Francisco, CA).

In situ hybridization

The technique previously described by Drayton et al. (19) was used. Briefly, fixed LNs were cut onto poly-L-lysine-coated slides and analyzed with the following digoxigenin (DIG)-labeled riboprobes: CCL21, CCL19, and CXCL13 sense and antisense probes. Signal was detected by overnight

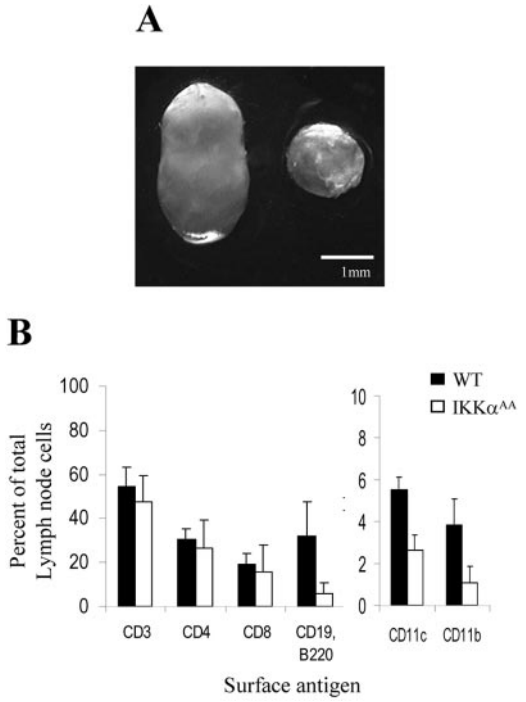

FIGURE 1. The LNs of IKKα^{AA} mice are reduced in size and cellular composition. *A*, The photograph of inguinal LNs from a WT littermate (*left*) and an IKKα^{AA} (*right*) mouse injected with Evans blue for LN visualization shows the presence of small LNs in IKKα^{AA} mice. *B*, WT and IKKα^{AA} LN cells were stained with the indicated PE- or FITC-conjugated Abs. The percentage of positive cells was determined by flow cytometry.

incubation of sections with alkaline-phosphatase-conjugated sheep anti-DIG Ab (Roche Diagnostic Systems, Mannheim, Germany) and was developed with NBT/5-bromo-4-chloro-3-indolyl phosphate (Invitrogen Life Technologies, Gaithersburg, MD).

Flow cytometric analysis

LN and thymic tissues were harvested from mice, homogenized in PBS, and passed over a 40-μm cell strainer (BD Biosciences, Bedford MA). Isolated cells were resuspended in FACS buffer (PBS supplemented with 1% FBS and 0.1% sodium azide). FACS staining was performed by conventional procedures using either FITC- or PE-conjugated anti-CD3, -CD4, -CD8, -B220, -CD19, -CD11c, -CD11b, and -CD62L Abs (all from BD Pharmingen). Data were collected on a FACSCalibur (BD Biosciences, San Jose, CA) flow cytometer and analyzed with FlowJo software (Tree Star, Ashland, OR).

Quantitative RT-PCR

Total RNA was prepared from WT and IKKα^{AA} LNs with an RNeasy kit (Qiagen, Valencia, CA) and treated with RNase-Free DNase set to remove residual genomic DNA (Qiagen). First strand cDNA was prepared using oligo(dT) primers and SuperScript II reverse transcriptase (Invitrogen Life Technologies). Samples were analyzed in triplicate with SYBR Green Master Mix (Qiagen). GAPDH was used as an endogenous control to determine relative expression of target genes. Data were collected using the ABI PRISM 7700 Sequence Detection System (Applied Biosystems, Foster City, CA). CCL21 and CXCL13 oligonucleotide primers have been previously described (8).

Results

Rudimentary LNs from IKKα^{AA} mice exhibit structural and cellular defects

Previous studies have established a role for IKKα kinase activity in PP and splenic development through analysis of IKKα^{AA} mutant mice (30). However, LN development has not been studied in detail. To further determine the contribution of IKKα to lymphoid organs, we investigated the presence of LNs in IKKα^{AA} mice by injection of Evans blue in the hind footpad. Upon initial macroscopic examination of untreated IKKα^{AA} mice, inguinal LNs appeared to be absent while the presence of other LNs, including the MLNs, was apparent. However, closer examination of Evans blue-injected animals revealed the presence of several other LNs, including inguinal LNs (Fig. 1*A*). Although all LNs analyzed (axillary, brachial, iliac, lumbar, inguinal, popliteal, cervical, and mesenteric) could be detected in IKKα^{AA} mice, they were smaller than those of wild-type (WT) mice (Fig. 1*A*) and exhibited reduced cellularity (Table I). Of the LNs examined, inguinal, axillary, and popliteal LNs exhibited the most striking reduction in size (Fig. 1*A*, and data not shown). Given the reduction in the size of IKKα^{AA} LNs, we next examined the cellular composition of these tissues by flow cytometric analysis (FACS). Quantitation of absolute cell number and FACS analysis of IKKα^{AA} LN cells revealed a reduction in total cellularity. All populations were affected (Fig. 1 and Table I) and, in fact, there was a large proportion of cells that did not react with standard phenotypic markers. Most notably, the proportion and number of mature B220$^+$CD19$^+$ B cells was markedly reduced (Fig. 1*B* and Table I). Although B220$^+$CD19$^+$ B cells comprised 40% of the total LN cells in WT controls, this population was reduced to 4% in IKKα^{AA} LNs. No significant differences in the proportion of CD4$^+$ and CD8$^+$ T cells were observed in WT and IKKα^{AA} LNs (Fig. 1*B*) or the thymus (data not shown). In addition to B cell defects, we also observed a reduction in the proportion and number of CD11c$^+$ dendritic cells and CD11b$^+$ macrophages in IKKα^{AA} LNs (Fig. 1*B* and Table I). This impaired LN cellular composition prompted us to investigate the contribution of IKKα^{AA} kinase activity to other hallmarks of normal LNs. Two-color immunofluorescence analysis of WT and IKKα^{AA} LNs revealed numerous defects in IKKα^{AA} LN microarchitecture. WT LNs exhibited T and B cell compartmentalization and prominent B cell follicles (Fig. 2). Consistent with the paucity of B cells revealed by flow cytometric analysis, IKKα^{AA} LNs were characterized by only a thin rim of B cells located in the LN cortex (Fig. 2). Further immunohistochemical analysis of the B cell compartment in these LNs with anti-CD35 revealed fewer and smaller follicular dendritic cell (FDC) networks than in WT controls (Fig. 2).

Table I. *Cellularity of WT and IKKα^{AA} PLNs*[a]

	Total Cell Number ($\times 10^6$)	CD4$^+$	CD8$^+$	CD19$^+$B220$^+$	CD11c$^+$	CD11b$^+$
WT PLN	12.83 ± 0.97	4.68 ± 0.58	3.17 ± 0.52	4.04 ± 1.10	0.72 ± 0.23	0.49 ± 0.26
IKKα^{AA} PLN	9.87 ± 2.11	2.11 ± 0.95	0.95 ± 0.19	0.33 ± 0.01	0.35 ± 0.21	0.15 ± 0.11

[a] Cells were isolated from WT and IKKα^{AA} PLNs. PLNs included pooled brachial and axillary LNs. Cells were first counted by trypan blue exclusion on a hemacytometer, the proportion of the indicated cell populations was determined by flow cytometry, and the absolute cell number was determined; (n = 3).

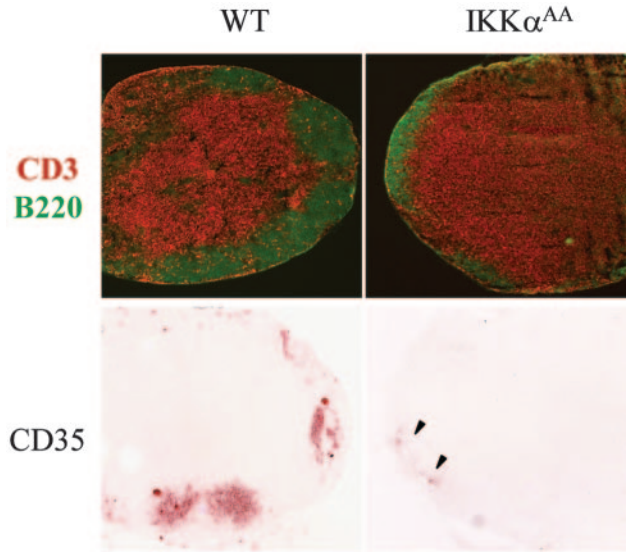

FIGURE 2. Defective tissue microarchitecture and FDC networks in IKKα^{AA} LNs. *Top panel*, Two-color immunofluorescence analysis with anti-CD3 PE (red) and anti-B220 FITC (green) reveals T and B cell compartmentalization in both WT and IKKα^{AA} LNs. However, IKKα^{AA} LN B cells occupied a thin rim in the LN cortex compared with the relatively large, distinct B cell follicles observed in WT littermate LNs. *Bottom panel*, Immunohistochemical analysis with anti-CD35 (CR-1) to detect FDCs networks reveals small FDCs clusters in IKKα^{AA} LN (arrowheads) compared with WT counterparts. Original objective, ×20.

Diminished stromal and HEV-specific lymphoid chemokine expression in IKKα^{AA} LNs

Having noted impaired follicle development and cellular recruitment to IKKα^{AA} LNs, we sought to identify a mechanism for this defect. In situ hybridization analysis for lymphoid chemokine expression (CCL19, CCL21, and CXCL13) revealed a substantial reduction in the accumulation of all three chemokine transcripts in IKKα^{AA} LNs when compared with WT LNs (Fig. 3*A*). Consistent with fewer B cells in IKKα^{AA} LNs, CXCL13 transcripts were significantly reduced and in some cases, undetectable by in situ hybridization analysis (Fig. 3*A*). Stromal expression of CCL21 and CCL19 was also reduced in IKKα^{AA} LNs (Fig. 3*A*). Moreover, HEV-specific CCL21 expression was greatly diminished (Fig. 3*A*, *inset*). Quantitative RT-PCR analysis revealed a respective 10- and 27-fold reduction in CCL21 and CXCL13 expression compared with WT controls (Fig. 3*B*).

IKKα kinase activity contributes to HEV gene expression and the generation of functional HEV ligands

Given a previously hypothesized role for LT$\alpha\beta$ and the alternative NF-κB pathway in HEV genesis (19), the hypocellularity of IKKα^{AA} LNs, and diminished CCL21 expression in IKKα^{AA} LN-HEV, we investigated the HEV phenotype in IKKα^{AA} PLNs. First, WT, TNFRI$^{-/-}$, LT$\beta^{-/-}$, and IKKα^{AA} LNs were analyzed by immunohistochemistry for GlyCAM-1 expression. In WT LN, GlyCAM-1 exhibited high HEV-specific expression (Fig. 4*A*). TNFRI$^{-/-}$ mice exhibited slightly reduced expression of GlyCAM-1 on LN-HEV (Fig. 4*B*). In contrast, both IKKα^{AA} and LT$\beta^{-/-}$ LN-HEV exhibited marked reductions in GlyCAM-1 expression (Fig. 4, *C* and *D*). Whereas low levels of GlyCAM-1 could be detected in IKKα^{AA} LNs, it was undetectable on LT$\beta^{-/-}$ MLN-HEV. Consistent with the marked reduction in the GlyCAM-1 protein, GlyCAM-1 mRNA transcripts were not detectable by in situ hybridization analysis in LT$\beta^{-/-}$ MLN-HEV, and in five of six (~83%) IKKα^{AA} mice, while one IKKα^{AA} mouse exhibited severely reduced GlyCAM-1 expression (data not shown).

To further examine the contribution of IKKα kinase activity to the HEV phenotype, we investigated PNAd, the HEV-borne CD62L ligand, and HEC-6ST expression by two-color immunofluorescence on WT, TNFRI$^{-/-}$, LT$\beta^{-/-}$, and IKKα^{AA} LNs. WT LN-HEV exhibited concomitant pericellular (i.e., luminal and abluminal) PNAd expression and high levels of HEC-6ST (Fig. 4, *E* and *I*). Analysis of TNFRI$^{-/-}$ LNs revealed a pattern of PNAd and HEC-6ST expression similar to that seen in WT controls, although a few small vessels displayed only abluminal PNAd expression

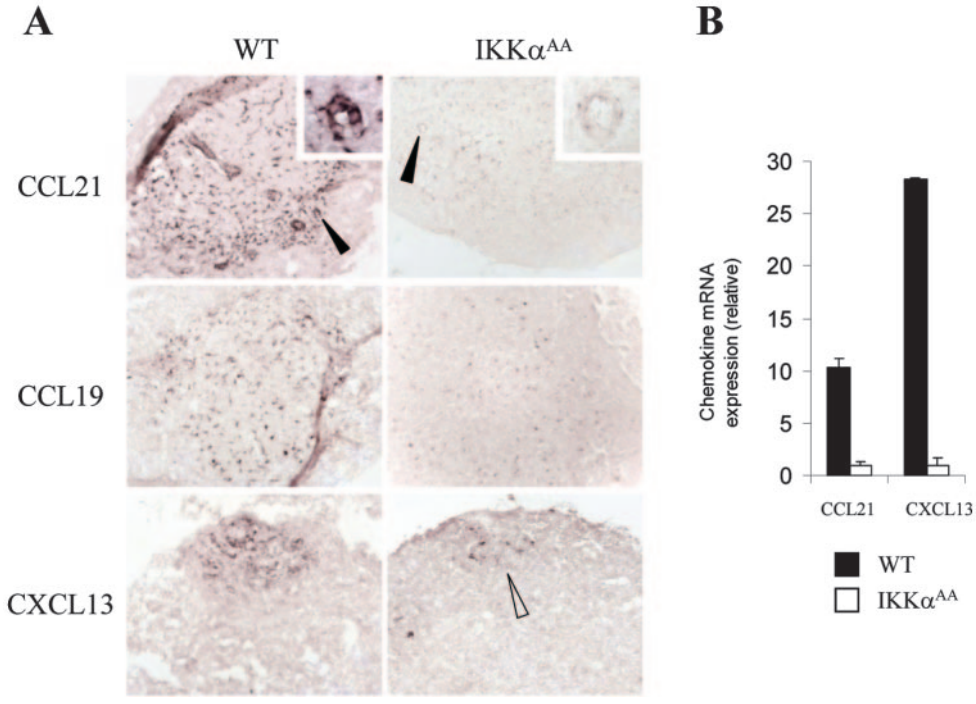

FIGURE 3. Lymphoid chemokine expression is diminished in IKKα^{AA} LNs. *A*, In situ hybridization analysis of WT littermate and IKKα^{AA} LNs with DIG-labeled anti-sense riboprobes to CCL21, CCL19, or CXCL13. Stromal expression of CCL21 and CCL19 and follicular expression of CXCL13 (open arrowhead) are dramatically reduced in IKKα^{AA} LNs. A high magnification *inset* (filled arrowhead) also reveals a marked reduction in CCL21 expression on IKKα^{AA} LN-HEV. Positive signal is seen as dark purple staining. Original objective, ×20. CCL21 *inset*, ×100. *B*, Real-time PCR of total RNA was extracted from WT and IKKα^{AA} LNs, reverse transcribed, and CCL21 and CXCL13 expression levels were monitored. CCL21 and CXCL13 mRNA expression is reported relative to GAPDH mRNA expression.

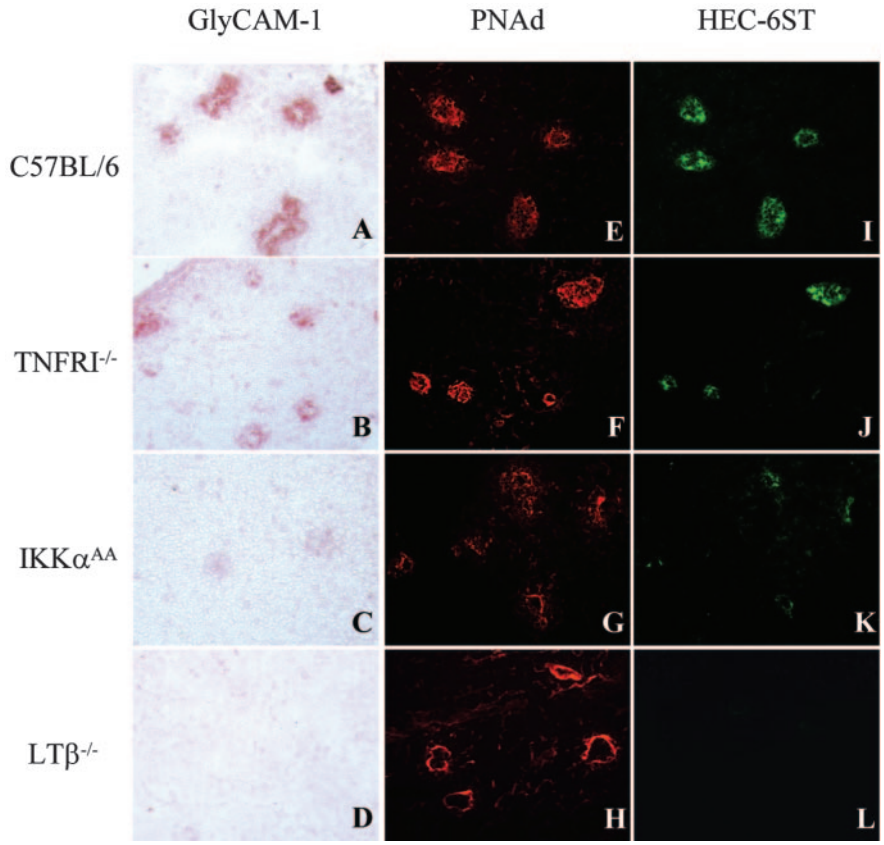

FIGURE 4. IKKα kinase activity is crucial for HEV-specific gene expression. WT, TNFRI$^{-/-}$, IKKα^{AA}, and LT$\beta^{-/-}$ LN sections were analyzed with Abs directed against GlyCAM-1, PNAd, and HEC-6ST. WT and TNFRI$^{-/-}$ LNs exhibited high HEV-specific expression of all markers, while IKKα^{AA} LN-HEV displayed reduced levels of all markers. LT$\beta^{-/-}$ LN-HEV exhibited undetectable GlyCAM-1 expression and a large proportion (40–50%) of the HEV exhibited only abluminal PNAd expression and a corresponding absence of HEC-6ST as previously described (19). Original objective, ×40.

with no detectable HEC-6ST (Fig. 4, *F* and *J*). The HEV phenotype in TNFRI$^{-/-}$ mice is the reciprocal of that seen in LT$\beta^{-/-}$ mice. Whereas TNFRI$^{-/-}$ mice exhibited predominately pericellular PNAd expression on HEV, we have previously shown that LT$\beta^{-/-}$ mice exhibit a higher proportion of HEV displaying only abluminal PNAd and a corresponding absence of HEC-6ST on these vessels (Fig. 4, *H* and *L*; Ref. 19). In contrast to WT and TNFRI$^{-/-}$ LN-HEV, IKKα^{AA} LN-HEV displayed an abnormal pattern of PNAd staining characterized by a lack of distinct pericellular PNAd expression (Fig. 4*G*) presumably due to the modification of other glycoproteins, such as CD34, by a sulfotransferase other than HEC-6ST as previously discussed (19, 20). Furthermore, HEC-6ST expression was markedly reduced compared with WT controls and TNFRI$^{-/-}$ mice (Fig. 4*K*). Consistent with diminished HEC-6ST expression on IKKα^{AA} LN-HEV, quantitative RT-PCR revealed a 4-fold reduction in this transcript compared with WT (data not shown).

Given diminished HEC-6ST expression and nearly undetectable GlyCAM-1 expression in IKKα^{AA} LN-HEV, we next examined CD62L^{high} cell recruitment to these LNs as an indicator of HEV function. We have previously reported that CD62L^{+} cell accumulation is reduced in LT$\beta^{-/-}$ MLN (19). Although the proportion of CD62L^{+} cells was similar in both WT, TNFRI$^{-/-}$, and IKKα^{AA} MLNs, the intensity of CD62L staining was reduced on only those cells isolated from IKKα^{AA} MLNs pointing to a reduction in functional CD62L on HEV (Fig. 5*A*, and data not shown). Whereas nearly 70% of WT MLN cells exhibited high CD62L expression, this population was dramatically reduced to 24% in IKKα^{AA} MLNs (Fig. 5*B*)

IKKα kinase activity is important for normal NALT organogenesis

We also investigated the involvement of IKKα in NALT development. Gross histology revealed the presence of this organ in both WT and IKKα^{AA} mice (Fig. 6). However, when compared with WT controls, IKKα^{AA} NALTs were reduced in size (Fig. 6, *A* and *E*). Whereas the WT NALT is characterized by a large proportion of B cells surrounded by a smaller ring of T cells (Fig. 6*B*), IKKα^{AA} NALTs exhibited marked structural disruptions including comingling of T and B cells (Fig. 6*F*). As was seen in the LN, both the number of T and B cells in the NALT appeared reduced but the effect was more pronounced with regard to B cells.

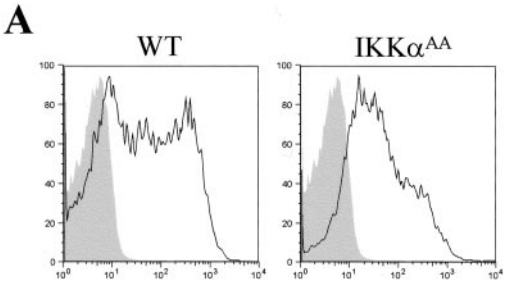

B

	WT	IKKα^{AA}
CD62L$^{int\text{-}hi}$	67.9 %	24.2 %
CD62L^{lo}	32.1 %	74.8 %

FIGURE 5. Reduced levels of CD62L expression on IKKα^{AA} LN cells. *A*, Flow cytometric analysis of WT and IKKα^{AA} MLN cells stained with anti-CD62L reveals a reduction in CD62L$^{int\text{-}high}$ cell accumulation in IKKα^{AA} MLN. *B*, The percentage of CD62L$^{int\text{-}high}$ and CD62L^{low} cells was determined from the total CD62L^{+} cells.

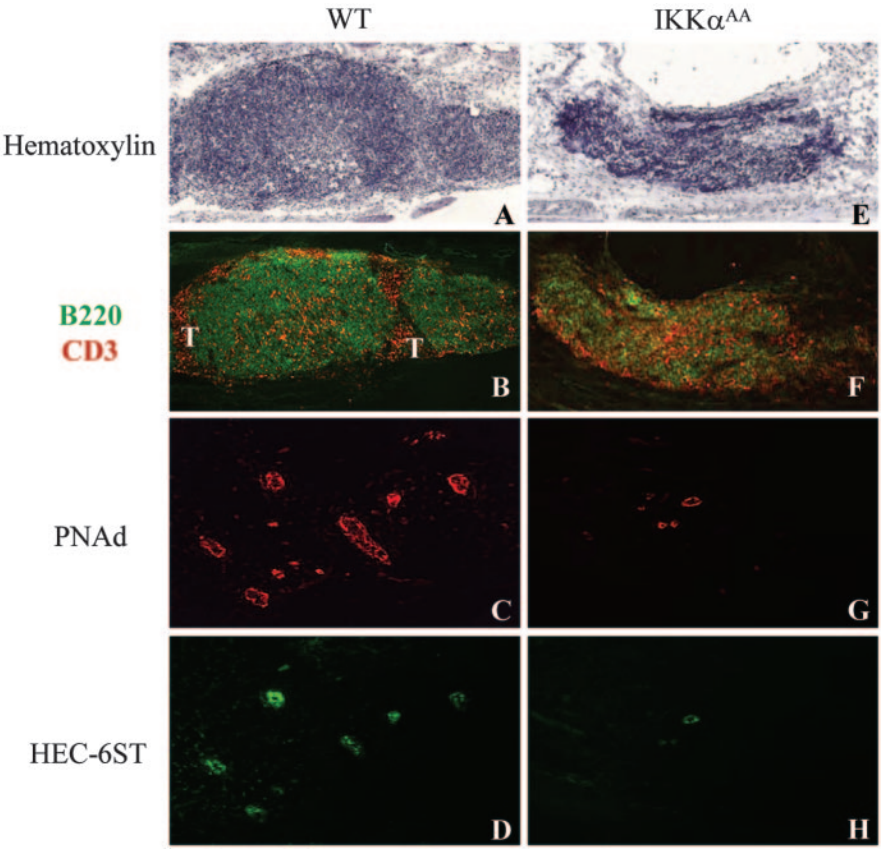

FIGURE 6. Impaired NALT organogenesis in IKKα^{AA} mice. *A* and *E*, Comparison of WT littermate and IKKα^{AA} NALT tissue stained with hematoxylin reveals reduction in the size of IKKα^{AA} NALT. *B* and *F*, Cellular compartmentalization of NALT tissue was analyzed by two-color immunofluorescence with anti-CD3 PE (red) and anti-B220 FITC (green). In WT NALT, a central area of B cells (green) is surrounded by a small ring of T cells (T, red) whereas the IKKα^{AA} NALT was characterized by an absence of distinct T and B cell compartments. *C–H,* HEV-specific gene expression is markedly reduced on IKKα^{AA} NALT-HEV. Fixed WT and IKKα^{AA} NALT tissue sections were double-stained with MECA 79 (anti-PNAd) and anti-HEC-6ST Abs to detect HEV. WT NALT-HEV exhibited high coexpression of PNAd and HEC-6ST while expression of these markers were severely reduced on IKKα^{AA} NALT-HEV. Original objective, ×20.

We next examined the NALT-HEV phenotype by two-color immunofluorescence. Similar to WT LN-HEV, WT NALT-HEV exhibited intense PNAd staining with coincidental HEC-6ST expression (Fig. 6, *C* and *D*). However, IKKα^{AA} NALT had few PNAd$^+$ HEV (Fig. 6*G*). These vessels were small with primarily abluminal PNAd staining compared with predominantly pericellular PNAd expression found in WT NALT. Similarly, HEC-6ST expression was dramatically reduced in IKKα^{AA} NALT-HEV (Fig. 6*H*).

LTβR is expressed on LN- and NALT-HEV

We have previously shown that LTβ, likely signaling through the LTβR, is important for the optimal expression of HEC-6ST and PNAd on HEV (19), and shown here with analysis of LT$\beta^{-/-}$ mice that GlyCAM-1 is also an LTβ target. Given that IKKα is a crucial component of LTβR signaling and that there were HEV defects in IKKα^{AA} LN and NALT tissue, we sought to determine whether LTβR was expressed on HEV to determine whether LTβR activity could contribute directly to HEV-specific gene expression. C57BL/6 LN and NALT tissue were analyzed by two-color immunofluorescence with MECA 79 (anti-PNAd) and anti-LTβR Abs (Fig. 7). Examination of LN and NALT tissue revealed prominent coexpression of both PNAd and LTβR on HEV. Interestingly, while PNAd$^+$LTβR$^+$ HEV were readily detected in both LN and NALT tissue, there are also some HEV that expressed only the LTβR, particularly in the NALT.

Discussion

In this paper, we have studied the contribution of IKKα, an essential component of the alternative NF-κB pathway, to LN and NALT organogenesis. By using IKKα^{AA} knockin mice, we provide evidence that IKKα activation and kinase activity contribute in a crucial manner to both LN and NALT organogenesis through regulation of tissue cellularity, organization, chemokine expression, and HEV development. IKKα^{AA} mice were characterized by the presence of small, hypocellular LN and NALT tissue exhibiting multiple structural defects. Although IKKα^{AA} kinase activity is not critical for T and B cell compartmentalization in the LN, it plays an important role in B cell follicle development and is also crucial for compartmentalization of the NALT. Furthermore, consistent with the hypothesis that signaling via the alternative NF-κB pathway regulates lymphoid chemokine expression (8), we find that IKKα^{AA} mice have severe defects in LN expression of CCL21, CCL19, and CXCL13. The reduced expression of these chemokines involved in the recruitment of lymphoid and myeloid cells to secondary lymphoid organs (33) may account, in part, for the reduced numbers of cells. Further analysis also revealed a previously unidentified role for IKKα in HEV development through regulation of HEV-specific gene expression. It is likely that impaired expression of HEV genes also contributes to the significant reduction in cell recruitment to IKKα^{AA} LN and NALT organs. It is of interest that CD62L expression on B cells is only half that of T cells, and that when CD62L expression is limited, reduced rolling is seen on HEV where CD62L ligand expression is also reduced (34). In previous reports, it has been noted that additional CD62L ligands probably exist (35, 36) and these ligands could bind cells expressing different levels of CD62L and could account for the entry of CD62L^{low} cells into IKKα^{AA} LNs. It is also possible that a different ligand/receptor pair could be used by these cells.

Numerous reports addressing the cellular and molecular interactions that govern secondary lymphoid organogenesis have demonstrated that LN, PP, and NALT each require a different set of signals for their development (7). For example, LTβR- and NIK-deficient mice lack all LNs and PP, yet retain NALT formation,

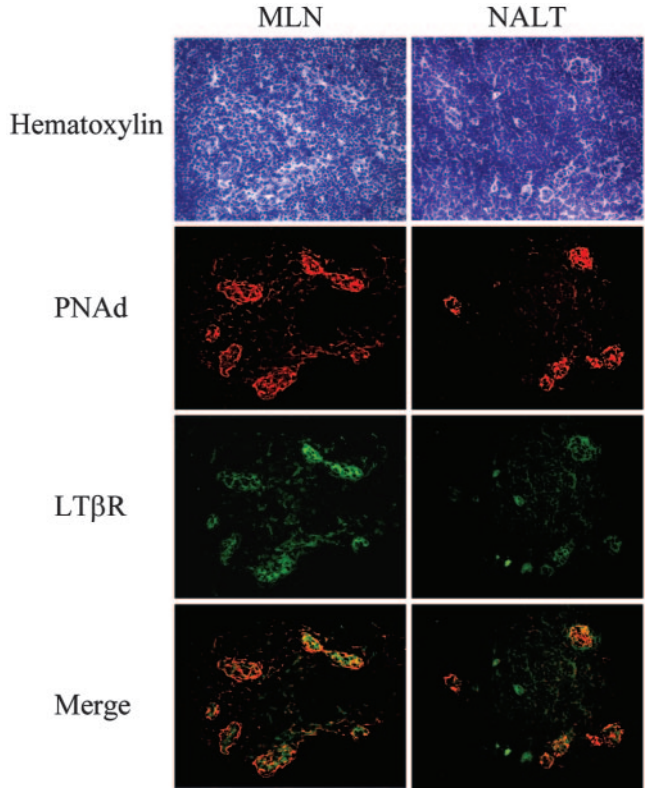

FIGURE 7. LTβR expression on HEV. WT LN and NALT tissue were analyzed by two-color immunofluorescence with MECA 79 (red) and anti-LTβR (green). Sections were counterstained with hematoxylin (*top panel*). LN- and NALT-HEV exhibited coincidental expression of PNAd and LTβR on most HEV. Objective, ×20.

suggesting that signaling via the alternative NF-κB pathway is not crucial for initiation of NALT development (29). In this study, we report that IKKα kinase activity is also dispensable for NALT formation but plays an important role in NALT maturation. Unlike LNs, which complete development during embryogenesis or shortly thereafter, the NALT continues to develop up to 6 wks after birth. Similar to LNs, IKKα kinase activity plays a crucial role in NALT architecture, cellularity, and HEV development.

We have previously described a role for LTαβ in HEV development through the regulation of PNAd and HEC-6ST expression and proposed that this regulation occurs through the LTβR→NIK→IKKα alternative NF-κB pathway (19). In support of this hypothesis, in this study, we show that IKKα is necessary for optimal PNAd and HEC-6ST expression on LN- and NALT-HEV. In addition, we demonstrate that a mechanism by which IKKα regulates the HEV phenotype is through regulation of GlyCAM-1, a core glycoprotein in the PNAd-generating pathway, and regulation of the lymphoid chemokine, CCL21. We also demonstrate that similar to IKKα, LTβ also regulates GlyCAM-1 expression in HEV. The observation that TNFRI$^{-/-}$ LNs have a slightly reduced expression of both HEC-6ST and GlyCAM-1 indicates that while the canonical NF-κB pathway may not play a primary role in HEV-specific gene expression, it does cooperate with the alternative NF-κB pathway in this process.

Although IKKα is crucial for LTβR signaling, we note it has also been implicated in signaling downstream of other receptors including CD40 (37), BAFF-R (38), and RANK (30). Therefore, it is conceivable that these other receptors also contribute to the secondary lymphoid organ defects observed in IKKα^{AA} mice. Because CD40 is necessary for the clonal expansion of B cells (39), and BAFF contributes to their maturation (40, 41), it is possible that the reduction in mature B cell cellularity in IKKα^{AA} LNs is due, in part, to a greater proportion of immature B cells. Nonetheless, the fact that LTβ$^{-/-}$ and IKKα^{AA} mice have overlapping defects in HEV further supports the notion that the LTβR→NIK→IKKα alternative NF-κB pathway regulates HEV-specific gene expression and plays a key role in LN and NALT organogenesis.

An interesting question is whether the HEV defects in IKKα^{AA} mice are a result of diminished IKKα activity in high endothelial cells and/or defective LN stromal cell signaling whose products affect the HEV phenotype. The most direct model for LTαβ and IKKα involvement in HEV-specific gene expression is that LTαβ binds to LTβR expressed on endothelial cells, engages the alternative NF-κB pathway, triggers IKKα activation and subsequent transcription of HEC-6ST, GlyCAM-1, and CCL21. Although LTβR expression has been detected on HUVEC cells (42), its expression on HEV had not been described previously. In this paper, we establish that LTβR is highly expressed on HEV in both the LN and NALT; a finding in support of the hypothesis that LTαβ can exert its effects directly on high endothelial cells. Future studies will address whether direct signaling via the LTβR on high endothelial cells in vivo regulates gene expression.

Targeted disruptions of alternative NF-κB pathway components including LTβ, LTβR, NIK, NF-κB2, and RelB, result in extensive defects in secondary lymphoid organogenesis (7, 24). The defects in IKKα^{AA} mice are not as severe as those seen in mice deficient in the upstream signaling molecule, NIK, in that IKKα^{AA} mice retain LN and NALT albeit these organs are defective. One possibility for the retention of small, rudimentary LNs and NALT tissue in IKKα^{AA} mice is that the IKKα^{AA} mutation only prevents inducible IKKα kinase activity but permits basal activity (13). However, as the phenotype of IKKα^{AA} mice is similar to that of mice deficient in downstream molecules of the alternative NF-κB pathway including NF-κB2 and RelB, the basal activity of the IKKα^{AA} variant must be very low. Most notably, NF-κB2$^{-/-}$ and IKKα^{AA} mice have strikingly similar LN defects—small, undeveloped LNs, defective follicle formation, and a marked reduction in B cell accumulation (24). Therefore, while IKKα kinase activity is not essential for initiation of LN and NALT organogenesis, it is crucial for later stages of development including HEV formation, lymphoid chemokine expression, and proper tissue microarchitecture.

Given the gross similarities between IKKα^{AA}, NF-κB2$^{-/-}$, and RelB$^{-/-}$ mice, a previously identified role for IKKα in LTβR activation of the alternative NF-κB pathway, and the normal activation of the canonical NF-κB pathway by TNF-α in IKKα^{AA} mice (8, 30), it is likely that the secondary lymphoid organ defects in IKKα^{AA} mice are attributable to abrogated activation of the alternative NF-κB pathway. However, the fact that LNs are not completely eliminated in IKKα^{AA}, NF-κB2$^{-/-}$, and RelB$^{-/-}$ mice suggests that components of the canonical pathway are also involved in this process. For example, molecules such as VCAM-1 and mucosal addressin cell adhesion molecule 1, induced by both TNFRI and LTβR through the canonical pathway, are also crucial for normal LN development (7). In addition, both the LTα:TNFRI and LTαβ:LTβR ligand:receptor pairs regulate lymphoid chemokine expression (8, 18). Therefore, while both NF-κB pathways differentially regulate gene expression, their activities likely cooperate in secondary lymphoid organogenesis and HEV development.

Acknowledgments

We thank Magali Bebien (University of California, San Diego) for her assistance, Dr. Louis Alexander (Department of Epidemiology and Public Health, Yale University) for use of the ABI PRISM Detection System, and

Dr. Steve Rosen (University of California, San Francisco) for the anti-GlyCAM-1 Ab.

References

1. Neumann, B., A. Luz, K. Pfeffer, and B. Holzmann. 1996. Defective Peyer's patch organogenesis in mice lacking the 55-kD receptor for tumor necrosis factor. *J. Exp. Med. 184:259*.
2. Pasparakis, M., L. Alexopoulou, M. Grell, K. Pfizenmaier, H. Bluethmann, and G. Kollias. 1997. Peyer's patch organogenesis is intact yet formation of B lymphocyte follicles is defective in peripheral lymphoid organs of mice deficient for tumor necrosis factor and its 55-kDa receptor. *Proc. Natl. Acad. Sci. USA 94:6319*.
3. Futterer, A., K. Mink, A. Luz, M. H. Kosco-Vilbois, and K. Pfeffer. 1998. The lymphotoxin β receptor controls organogenesis and affinity maturation in peripheral lymphoid tissues. *Immunity 9:59*.
4. De Togni, P., J. Goellner, N. H. Ruddle, P. R. Streeter, A. Fick, S. Mariathasan, S. C. Smith, R. Carlson, L. P. Shornick, J. Strauss-Schoenberger, et al. 1994. Abnormal development of peripheral lymphoid organs in mice deficient in lymphotoxin. *Science 264:703*.
5. Banks, T. A., B. T. Rouse, M. K. Kerley, P. J. Blair, V. L. Godfrey, N. A. Kuklin, D. M. Bouley, J. Thomas, S. Kanangat, and M. L. Mucenski. 1995. Lymphotoxin-α-deficient mice: effects on secondary lymphoid organ development and humoral immune responsiveness. *J. Immunol. 155:1685*.
6. Korner, H., M. Cook, D. S. Riminton, F. A. Lemckert, R. M. Hoek, B. Ledermann, F. Kontgen, B. Fazekas de St. Groth, and J. D. Sedgwick. 1997. Distinct roles for lymphotoxin-α and tumor necrosis factor in organogenesis and spatial organization of lymphoid tissue. *Eur. J. Immunol. 27:2600*.
7. Mebius, R. E. 2003. Organogenesis of lymphoid tissues. *Nat. Rev. Immunol. 3:292*.
8. Dejardin, E., N. M. Droin, M. Delhase, E. Haas, Y. Cao, C. Makris, Z. W. Li, M. Karin, C. F. Ware, and D. R. Green. 2002. The lymphotoxin-β receptor induces different patterns of gene expression via two NF-κB pathways. *Immunity 17:525*.
9. Ghosh, S., and M. Karin. 2002. Missing pieces in the NF-κB puzzle. *Cell 109: S81*.
10. Delhase, M., M. Hayakawa, Y. Chen, and M. Karin. 1999. Positive and negative regulation of IκB kinase activity through IKKβ subunit phosphorylation. *Science 284:309*.
11. Yamaoka, S., G. Courtois, C. Bessia, S. T. Whiteside, R. Weil, F. Agou, H. E. Kirk, R. J. Kay, and A. Israel. 1998. Complementation cloning of NEMO, a component of the IκB kinase complex essential for NF-κB activation. *Cell 93:1231*.
12. Tanaka, M., M. E. Fuentes, K. Yamaguchi, M. H. Durnin, S. A. Dalrymple, K. L. Hardy, and D. V. Goeddel. 1999. Embryonic lethality, liver degeneration, and impaired NF-κB activation in IKK-β-deficient mice. *Immunity 10:421*.
13. Senftleben, U., Y. Cao, G. Xiao, F. R. Greten, G. Krahn, G. Bonizzi, Y. Chen, Y. Hu, A. Fong, S. C. Sun, and M. Karin. 2001. Activation by IKKα of a second, evolutionary conserved, NF-κB signaling pathway. *Science 293:1495*.
14. Matsushima, A., T. Kaisho, P. D. Rennert, H. Nakano, K. Kurosawa, D. Uchida, K. Takeda, S. Akira, and M. Matsumoto. 2001. Essential role of nuclear factor (NF)-κB-inducing kinase and inhibitor of κB (IκB) kinase α in NF-κB activation through lymphotoxin β receptor, but not through tumor necrosis factor receptor I. *J. Exp. Med. 193:631*.
15. Muller, J. R., and U. Siebenlist. 2003. Lymphotoxin β receptor induces sequential activation of distinct NF-κB factors via separate signaling pathways. *J. Biol. Chem. 278:12006*.
16. Yin, L., L. Wu, H. Wesche, C. D. Arthur, J. M. White, D. V. Goeddel, and R. D. Schreiber. 2001. Defective lymphotoxin-β receptor-induced NF-κB transcriptional activity in NIK-deficient mice. *Science 291:2162*.
17. Shinkura, R., K. Kitada, F. Matsuda, K. Tashiro, K. Ikuta, M. Suzuki, K. Kogishi, T. Serikawa, and T. Honjo. 1999. Alymphoplasia is caused by a point mutation in the mouse gene encoding NF-κB-inducing kinase. *Nat. Genet. 22:74*.
18. Ngo, V. N., H. Korner, M. D. Gunn, K. N. Schmidt, D. S. Riminton, M. D. Cooper, J. L. Browning, J. D. Sedgwick, and J. G. Cyster. 1999. Lymphotoxin α/β and tumor necrosis factor are required for stromal cell expression of homing chemokines in B and T cell areas of the spleen. *J. Exp. Med. 189:403*.
19. Drayton, D. L., X. Ying, J. Lee, W. Lesslauer, and N. H. Ruddle. 2003. Ectopic LTαβ directs lymphoid organ neogenesis with concomitant expression of peripheral node addressin and a HEV-restricted sulfotransferase. *J. Exp. Med. 197:1153*.
20. Hemmerich, S., A. Bistrup, M. S. Singer, A. van Zante, J. K. Lee, D. Tsay, M. Peters, J. L. Carminati, T. J. Brennan, K. Carver-Moore, et al. 2001. Sulfation of L-selectin ligands by an HEV-restricted sulfotransferase regulates lymphocyte homing to lymph nodes. *Immunity 15:237*.
21. Cuff, C. A., J. Schwartz, C. M. Bergman, K. S. Russell, J. R. Bender, and N. H. Ruddle. 1998. Lymphotoxin α_3 induces chemokines and adhesion molecules: insight into the role of LTα in inflammation and lymphoid organ development. *J. Immunol. 161:6853*.
22. Sacca, R., C. A. Cuff, W. Lesslauer, and N. H. Ruddle. 1998. Differential activities of secreted lymphotoxin-α_3 and membrane lymphotoxin-$\alpha_1\beta_2$ in lymphotoxin-induced inflammation: critical role of TNF receptor 1 signaling. *J. Immunol. 160:485*.
23. Cuff, C. A., R. Sacca, and N. H. Ruddle. 1999. Differential induction of adhesion molecule and chemokine expression by $LT\alpha_3$ and LTαβ in inflammation elucidates potential mechanisms of mesenteric and peripheral lymph node development. *J. Immunol. 162:5965*.
24. Weih, F., and J. Caamano. 2003. Regulation of secondary lymphoid organ development by the nuclear factor-κB signal transduction pathway. *Immunol. Rev. 195:91*.
25. Weih, F., D. Carrasco, S. K. Durham, D. S. Barton, C. A. Rizzo, R. P. Ryseck, S. A. Lira, and R. Bravo. 1995. Multiorgan inflammation and hematopoietic abnormalities in mice with a targeted disruption of RelB, a member of the NF-κB/Rel family. *Cell 80:331*.
26. Hu, Y., V. Baud, M. Delhase, P. Zhang, T. Deerinck, M. Ellisman, R. Johnson, and M. Karin. 1999. Abnormal morphogenesis but intact IKK activation in mice lacking the IKKα subunit of IκB kinase. *Science 284:316*.
27. Takeda, K., O. Takeuchi, T. Tsujimura, S. Itami, O. Adachi, T. Kawai, H. Sanjo, K. Yoshikawa, N. Terada, and S. Akira. 1999. Limb and skin abnormalities in mice lacking IKKα. *Science 284:313*.
28. Kuper, C. F., P. J. Koornstra, D. M. Hameleers, J. Biewenga, B. J. Spit, A. M. Duijvestijn, P. J. van Breda Vriesman, and T. Sminia. 1992. The role of nasopharyngeal lymphoid tissue. *Immunol. Today 13:219*.
29. Fukuyama, S., T. Hiroi, Y. Yokota, P. D. Rennert, M. Yanagita, N. Kinoshita, S. Terawaki, T. Shikina, M. Yamamoto, Y. Kurono, and H. Kiyono. 2002. Initiation of NALT organogenesis is independent of the IL-7R, LTβR, and NIK signaling pathways but requires the Id2 gene and $CD3^{-}CD4^{+}CD45^{+}$ cells. *Immunity 17:31*.
30. Cao, Y., G. Bonizzi, T. N. Seagroves, F. R. Greten, R. Johnson, E. V. Schmidt, and M. Karin. 2001. IKKα provides an essential link between RANK signaling and cyclin D1 expression during mammary gland development. *Cell 107:763*.
31. Koni, P. A., R. Sacca, P. Lawton, J. L. Browning, N. H. Ruddle, and N. H. Flavell. 1997. Distinct roles in lymphoid organogenesis for lymphotoxins α and β in lymphotoxin β-deficient mice. *Immunity 6:491*.
32. Heritage, P. L., B. J. Underdown, A. L. Arsenault, D. P. Snider, and M. R. McDermott. 1997. Comparison of murine nasal-associated lymphoid tissue and Peyer's patches. *Am. J. Respir. Crit. Care Med. 156:1256*.
33. Muller, G., and M. Lipp. 2003. Concerted action of the chemokine and lymphotoxin system in secondary lymphoid-organ development. *Curr. Opin. Immunol. 15:217*.
34. Gauguet, J. M., S. D. Rosen, J. D. Marth, and U. H. von Andrian. 2004. Core 2 branching β1,6-*N*-acetylglucosaminyltransferase and high endothelial cell *N*-acetylglucosamine-6-sulfotransferase exert differential control over B and T lymphocyte homing to peripheral lymph node. *Blood. In press.*
35. Kanda, H., T. Tanaka, M. Matsumoto, E. Umemoto, Y. Ebisuno, M. Kinoshita, M. Noda, R. Kannagi, T. Hirata, T. Murai, et al. 2004. Endomucin, a sialomucin expressed in high endothelial venules, supports L-selectin-mediated rolling. *Int. Immunol. 16:1265*.
36. M'Rini, C., G. Cheng, C. Schweitzer, L. L. Cavanagh, R. T. Palframan, T. R. Mempel, R. A. Warnock, J. B. Lowe, E. J. Quackenbush, and U. H. von Andrian. 2003. A novel endothelial L-selectin ligand activity in lymph node medulla that is regulated by α(1,3)-fucosyltransferase-IV. *J. Exp. Med. 198:1301*.
37. Coope, H. J., P. G. Atkinson, B. Huhse, M. Belich, J. Janzen, M. J. Holman, G. G. Klaus, L. H. Johnston, and S. C. Ley. 2002. CD40 regulates the processing of NF-κB2 p100 to p52. *EMBO J. 21:5375*.
38. Claudio, E., K. Brown, S. Park, H. Wang, and U. Siebenlist. 2002. BAFF-induced NEMO-independent processing of NF-κB2 in maturing B cells. *Nat. Immunol. 3:958*.
39. Kehry, M. R. 1996. CD40-mediated signaling in B cells: balancing cell survival, growth, and death. *J. Immunol. 156:2345*.
40. Thompson, J. S., S. A. Bixler, F. Qian, K. Vora, M. L. Scott, T. G. Cachero, C. Hession, P. Schneider, I. D. Sizing, C. Mullen, et al. 2001. BAFF-R, a newly identified TNF receptor that specifically interacts with BAFF. *Science 293:2108*.
41. Schiemann, B., J. L. Gommerman, K. Vora, T. G. Cachero, S. Shulga-Morskaya, M. Dobles, E. Frew, and M. L. Scott. 2001. An essential role for BAFF in the normal development of B cells through a BCMA-independent pathway. *Science 293:2111*.
42. Mackay, F., G. R. Majeau, P. S. Hochman, and J. L. Browning. 1996. Lymphotoxin β receptor triggering induces activation of the nuclear factor κB transcription factor in some cell types. *J. Biol. Chem. 271:24934*.